ELSEVIER

Thin-film polymerization and 'RIS' Metropolis Monte Carlo simulation of fluorinated aromatic copoly(ester–amide)s

May May Teoh[a], Tai-Shung Chung[a],*, David A. Schiraldi[b], Si-Xue Cheng[c]

[a]*Department of Chemical and Environmental Engineering, National University of Singapore, 10 Kent Ridge Crescent, Singapore 119260, Singapore*
[b]*Department of Macromolecular Science, Case Western Reserve University, Cleveland, OH 44106, USA*
[c]*Department of Chemistry, Wuhan University, Wuhan 430072, People's Republic of China*

Abstract

In this study, wholly aromatic main chain copoly(ester–amide)s containing tetrafluorophthalic acid (TFPA-*ortho*), tetrafluoroisophthalic acid (TFIA-*meta*) and tetrafluoroterephthalic acid (TFTA-*para*) were synthesized to study the effects of kinks on the formation of mesophase and crystal texture. The effects of kink moieties on these copoly(ester–amide)s were also investigated by the 'RIS' metropolis Monte Carlo simulation. Computational results indicate that all systems form thermotropic liquid crystalline polymers (LCPs) because the calculated persistence ratios for the *ortho*-, *meta*- and *para*-linkage systems are 6.51, 7.64 and 10.49, respectively. Both simulation and experimental results agree that ABA/AAA/TFTA (*para*) system has the greatest tendency to yield the liquid crystal (LC) phase due to its greater persistence ratio, linearity, and chain stiffness. The incorporation of TFPA (*ortho*) moiety can effectively reduce 30% of the molar stiffness function and 23% of the persistence length as compared to those of the TFTA (*para*) system. Yet, the ABA/AAA/TFPA system may form LC texture because of its large, rigid, disk-like TFPA moiety and the crankshaft structure induced by *cis*-configuration between AAA and TFPA moieties. The *meta*-linkage system has a slower LC growth rate, but it has a much higher tendency to form LC than the *ortho*-linkage. Both *meta*- and *para*-linkage systems have close critical ABA content to form LC texture. When comparing the requirements of critical ABA content between ABA/AAA/TFIA and ABA/AAA/IA (isophthalic acid) systems, we surprisingly observed that the former has a much lower critical ABA content than the latter. The four fluorine substituents of TFIA definitely help chain rigidity and stabilize the LC mesogens. Even though these fluorinated moieties exhibit different conformations and configurations, they yield similar end-stage crystalline structure. The spherulites are grown from the dark brushes around a single disclination, indicating that these are the lowest energy for crystallization.
© 2005 Elsevier Ltd. All rights reserved.

Keywords: Fluorinated LCPs; Persistence ratio; Effects of kink linkage

1. Introduction

For more than two decades, main chain thermotropic liquid crystalline polymers (MCLCPs), both wholly rigid rod systems and those that incorporate flexible spacers, have been a subject of intensive investigation. The effects of various structural variations such as lateral substitutions, molecular kinks, flexible bonds, lateral groups, comonomer incorporation, etc. have been examined as an approach to decrease the functional characteristics of high melting points and facilitate processing [1–4]. Molecular blends of MCLCPs and conventional polymers also impart the resulting materials with enhanced properties [5]. Usually, the formation of liquid crystal (LC) morphological heterogeneity depends on the chain rigidity, aspect ratio, chemical structure, conformation and configuration. Thus, the physical and chemical properties of the newly added moieties strongly affect the LC stability of the resultant polymers.

Introduction of kink spacers linking the mesogenic groups has been heavily studied in recent years. The introduction of kink moieties into stiff rod-like LCPs is usually used to reduce melting points and offset the linearity of the rigid main chain [3,4,6]. For example, the decomposition temperatures (T_d) of terephthalic acid (TA)—is lower than its melting temperature (T_m),

---

eliminating the possibility of melt processing of such materials. Therefore, *ortho*- and *meta*-linked 'kinked' units are usually incorporated into the polymer main chain to decrease T_m, and to decrease the glass transition temperature (T_g) by reducing the rigidity of the polymer chains. The other potential result of kink unit incorporation is the significant reduction of polymer crystallinity. Such modification adversely affects the strength and rigid-rod character of the resultant polymers and unfavourably influences the stability of liquid crystalline phases.

Although many attempts have been employed to study liquid crystalline heterogeneity, such as (1) the characteristics of resultant LPCs through experiments, [7–9] and (2) chain rigidity and persistence ratio by computational simulation [10–13], the direct comparison of both experimental data and computational simulations are very limited. Additionally, when synthesizing new LCPs, little information is available about their structures and properties. Computational simulations can be a powerful tool which provides insights into structure. The Flory lattice model is commonly applied to LC systems, and supported the importance of molecular structure/geometry to the induction of liquid crystallinity [13,14]. According to Flory and Ronca, the critical axial ratio value of the rod molecules thermotropic liquid crystallinity is 6.42 [15]. Thus, LCPs which have a persistence ratio greater than 6.42 tend to form stable mesophases.

Since, aromatic main-chain poly(ester–amide)s represent an important family of commercial thermotropic LCPs, our research group has carried out systematical thin-film polymerization study on these copolymers, and examined their morphological changes, reaction kinetics, characterization as well as product surface energy [16–20]. It has been found that the *para*-linked poly(ester–amide)s have the highest tendency to form liquid crystalline materials. Surprisingly, *ortho*-linked LCPs have a higher tendency than *meta*-linked LCPs to exhibit a thermotropic liquid crystalline phase, as a result of low melting point and chain

flexibility [17]. Fluorinated liquid crystals have received attention for many years. Families of materials that have been studied generally include: (1) fluorinated LCPs with lateral substituents such as –CF$_3$ and –F as a ring substitution [21–23], or (2) alternative fluorocarbon–hydrocarbon segments, –(CH$_2$)$_m$–(CF$_2$)$_n$– [24–26] as side-chain/main-chain LCPs. To our best knowledge, only one study of LCPs synthesized by both fluorinated *ortho*- and *meta*-aromatic moieties on the main chain LCPs has been reported [18].

Our approach is to incorporate three monomeric monomers and randomly distribute them along the backbone, leading to an irregular chain structure and thus inhibiting regular chain packing for crystallization [1–4,6]. The purpose of the present study is to examine the effects of fluorinated kink moieties (*ortho*- and *meta*-linkage) on the persistence ratio and the generation of liquid crystallinity as well as crystallization state, using both experimental and computational simulation. In addition, the impact of kink moieties (*ortho* and *meta*) on the fully hydrogenated and fluorinated LC formation will also be explored. The LCPs polymerizations were conducted using the in situ thin-film polymerization and the molecular modeling was carried out using the 'RIS' metropolis Monte Carlo simulation. This study would reveal the important relationship between liquid crystalline heterogeneity and chain rigidity, as well as persistence ratio and chemical structure.

2. Experimental

2.1. Monomers

The monomers selected for this study are shown in Fig. 1. *p*-Acetoxybenzoic acid (ABA) was synthesized by acetylating *p*-hydroxybenzoic acid (*p*-HBA) with acetic anhydride in the presence of the catalyst, pyridine. The monomer, ABA was purified by a recrystallization process
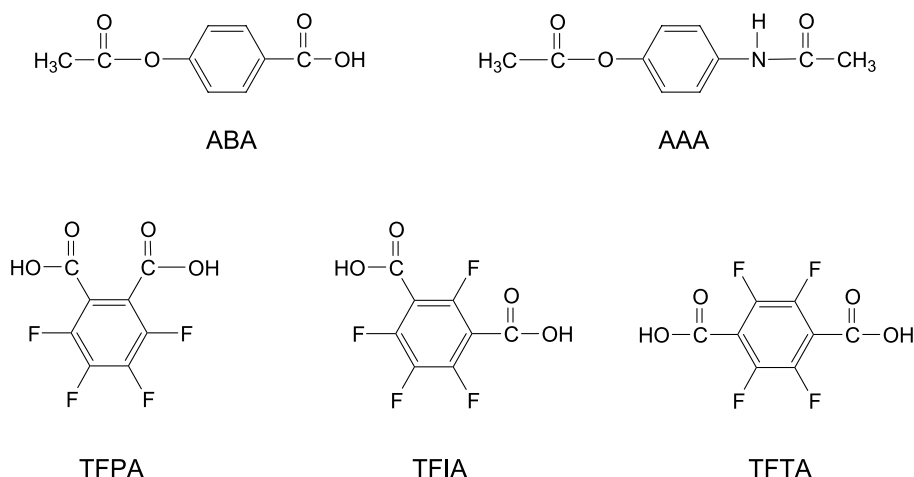

Fig. 1. Chemical structures of the monomers.

in butyl acetate. Acetoxy acetanilide (AAA) was also acetylated by *p*-aminophenol with acetic anhydride in a NaOH solution at low temperatures, recrystallized from (50/50 volume) methanol/hexane. The success of acetylation was confirmed by ^{1}H NMR spectroscopy. Tetrafluorophthalic acid (TFPA), tetrafluoroisophthalic acid (TFIA), and tetrafluoroterephthalic acid (TFTA) were purchased from Aldrich and used as received. The melting points for ABA, AAA, TFPA, TFIA, and TFTA are 196, 157, 162, 212, and 275 °C, respectively, as measured by differential scanning calorimetry (Perkin–Elmer DSC Pyris 1).

2.2. Thin film polymerization

The sample preparation began with the physical mixing of the monomers and grinding them together according to a specific molar ratio to obtain a homogenous mixture. Then, the monomer mixture was centrally placed on a microscopy cover slide. One drop of acetone was placed on the slide to dissolve the monomers. After the solvent evaporated, it left a thin layer of monomer mixture coating on the glass slide. The thickness of the specimens were within 5–10 μm. Next, the thin film layer was sandwiched between two glass slides using a 0.5 mm stainless steel ring spacer while the reactants were placed on the top cover slide. The ring spacer provided the space for the removal or release of acetic acid during polymerization. Without the spacer, it was found that the experimental reproducibility was quite low and micrograph

quality poor due to the vigorous evaporation (or release) of acetic acid at elevated temperature.

The specimen was placed on the heating stage (Linkam THMS-600) of a polarizing light microscope (Olympus BX50). The heating rate was raised to 90 °C/min at the desired temperature and the time measurement was started once the desired temperature was reached. During the in situ polymerization, the images of morphological changes were recorded and analyzed by imaging software (Image-Pro Plus 3.0). The detailed description of experimental procedures for the in situ thin film polymerization has been published elsewhere [7,16–20].
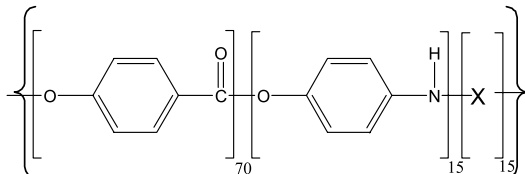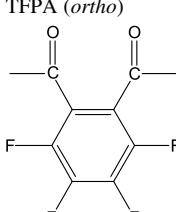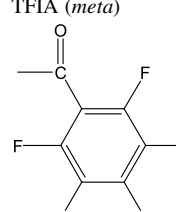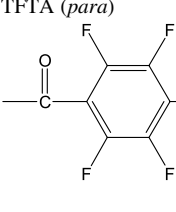
2.3. RMMC (the 'RIS' metropolis Monte Carlo method), Cerius[2] computational simulation

A RMMC (the 'RIS' metropolis Monte Carlo method) module within the Cerius[2] molecular simulation software for material science was used to calculate the properties of polymer chains, such as the mean-squared end-to-end distance, mean-squared radius of gyration, persistence length, and molar stiffness function of the polymer chains [27]. The most advanced polymeric force field, *pcff* (polymer consistent force field), was used for all systems. In addition to van der Waals interactions, electrostatic (Coulombic) and torsion interactions were included in RMMC simulation. During calculations, 500,000 steps were used in the equilibrium portion while 3,000,000 steps were

Table 1
The properties of the random built LCPs chains with *ortho*-, *meta*- and *para*-linkages (300 repeated units) at the temperature of 300 °C, simulated by RMMC-Cerius[2] molecular simulation software

Properties of polymer chains			
	TFPA (*ortho*)	TFIA (*meta*)	TFTA (*para*)
Mean squared end-to-end distance, $\langle r^2 \rangle$ (Å^2)	$81{,}749 \pm 4660$	$96{,}746 \pm 5340$	$131{,}934 \pm 6620$
Mean squared radius of gyration, $\langle s^2 \rangle$ (Å^2)	$14{,}023 \pm 95.8$	$15{,}811 \pm 112$	$20{,}820 \pm 135$
$\langle r^2 \rangle / \langle s^2 \rangle$	5.85	6.13	6.33
Persistence length (Å)	38.85 ± 2.33	44.72 ± 2.51	50.59 ± 2.87
Diameter (Å)	5.97 ± 0.34	5.85 ± 0.29	4.82 ± 0.25
Persistence ratio	6.51	7.64	10.49
Molar stiffness function ($\text{g}^{0.25}\,\text{cm}^{1.5}/\text{mol}^{0.75}$)	113.46	128.48	162.4

used in the production portion of the 'RIS' metropolis Monte Carlo simulation.

2.4. Fourier transform infrared spectroscopy (FT-IR) characterization

The monomers and polymers (in KBr pellets) were characterized by FT-IR (Perkin–Elmer FT-IR Spectrometer Spectrum 2000) with a wave number range of 4000–400 cm^{-1} and a resolution of 4 cm^{-1}. The polymers obtained by the thin film polymerization were scraped carefully from the glass slides without further treatment.

2.5. Differential scanning calorimetry (DSC)

The thin film polymerization product was tested by using a Perkin–Elmer Pyris-1 differential scanning calorimetry (DSC). The temperature range chosen in this work was from 50 to 380 °C. The normal heating rate is 20 °C/min. The sample was prepared by scraping the thin film polymerization product from the glass slide directly without any further treatment.

2.6. Thermo-gravimetric analysis (TGA)

The thermal decomposition studies were performed over a temperature range of 100–800 °C using a Perkin–Elmer TOA-7 under a nitrogen environment.

3. Results and discussion

3.1. Computational simulation

Table 1 summarizes the calculated results of polymer chain properties for the ABA/AAA/TFPA (TFIA/TFTA) system with different kinked effects. The polymers were built by the random polymer builder and the molar ratio of the simulation was 70:15:15 with 300 repeat units. Ten conformations of polymer chains were built for the particular LCPs chains and the results were averaged from these calculations. This was due to the fact that the Cerius^2 random polymer builder determined one probability of the given bond setting based on the relative energy of that particular setting in each calculation. The output from the metropolis Monte Carlo simulation, such as the persistence length and mean-square end-to-end distance were just one possible conformation sequence amongst many at one particular reaction temperature. However, if many chains are built, it is possible to determine the average polymer properties.

Although an isolated polymer chain is built by RMMC, the software has the capability to imitate as well as match experimental properties as close as possible. The force field, *pcff* (polymer consistent force field), within the RMMC simulation software, has taken the effects of other molecules

or solvents into consideration during the energy calculation. In other words, it uses 'the potentials of mean force' that has considered the polymer conformation in the present of other chains [27]. Previous study suggested that 200,000 steps were used in the equilibrium portion while 1,000,000 steps were used in the production portion [10]. Nevertheless, we intend to increase the equilibrium portion to 500,000 steps and production portion to 3,000,000 steps for a more precise calculation.

From the simulation results, ABA/AAA/TFTA (*para*) is predicted to have the highest persistence length, followed by ABA/AAA/TFIA (*meta*) and finally the ABA/AAA/TFPA (*ortho*) system. As expected, the *para*-linkage has the highest persistence length and ratio, which favours mesophase formation [17]. Moreover, the mean-squared end-to-end distance, mean-squared radius of gyration and molar stiffness function also increase linearly in this sequence: *ortho*-, *meta*- and lastly, *para*-linkage. According to the Flory's lattice model, the critical axial ratio value of the rod-like thermotropic liquid crystallinity is 6.42 [15]. In the current study, the calculated persistence ratios for the ABA/AAA/fluorinated aromatic copoly(ester–amide)s systems with *ortho*-, *meta*- and *para*-linkage are 6.51, 7.64 and 10.49, respectively. These results clearly support the formation of thermotropic LCPs. Based on the Odijk's presumption, the splay, twist, and bend elastic constants increase with an increase in persistence length or persistence ratio [28,29], indicating that the examined LCPs with a greater persistence ratio may exhibit strong LC characteristics.

The ABA/AAA/TFTA system with its *para*-linkage having the highest persistence ratio and persistence length easily undergoes the mesophase annihilation reaction. This may be explainable because the reactivity and chain straightness of TFTA are higher than TFIA/TFPA units, which may result in some blockiness in the polymer chain. Additionally, the chain orientation and packing are prevented to some extent by two symmetrical carbonyl groups that present in the linear TFTA unit. In other words, TFTA has a greater degree of linear symmetry that results in higher packing density. This is clearly supported by the conformational chain which is shown in Fig. 2(c). Remarkably, the persistence ratio and molar stiffness function of the ABA/AAA/TFTA system is the highest among the systems studied. These features are energetically favoured to form the liquid crystal or crystal structure.

The incorporation of the TFPA (*ortho*) unit can effectively reduce 30% of the molar stiffness function and 23% of the persistence length as compared to the TFTA (*para*) system, as shown in Table 1. Shibaev and Lam attributed the decrease in persistence ratio by the introduction of flexible sequences to the formation of Khun-like chains [14]. However, the TFPA monomer with its bulky structure (diameter of 5.97 Å) also significantly causes the reduction of persistence ratio. Thus, for a given persistence length, the *ortho*-isomers always have a lower persistence

ratio than the other two isomers. In addition, the lower intramolecular attractive force and high polarity in *ortho*-linkages may disturb the stability of the LC phase. Yet, the ABA/AAA/TFPA system may form LC texture because of its large, rigid, disk-like TFPA aromatic rings.

The calculated value of $\langle r^2 \rangle / \langle s^2 \rangle$ may provide additional insight because it describes the spatial characteristics of polymer chains. $\langle r^2 \rangle$ is the mean-squared end-to-end distance, while $\langle s^2 \rangle$ is the mean-squared radius of gyration. Therefore, the value of $\langle r^2 \rangle / \langle s^2 \rangle$ can be used to characterize the linearity of polymer. The higher the $\langle r^2 \rangle / \langle s^2 \rangle$ value, the more linear the polymer chain is. The calculated $\langle r^2 \rangle / \langle s^2 \rangle$ increases from kink to straight monomeric units, indicating that (1) the polymer chains form a worm-like structure with the *ortho-* and *meta-* linkages in the rigid-rod backbone or (2) excess electronegative fluorine charge may result in an increase in the interstitial space among polymer chains. The effects of the incorporation of rigid kinks in the polymer chains on the reduction of chain orientation can be easily seen from Table 1 and Fig. 2.

As illustrated in Fig. 2, the chain conformations of the *ortho-* and *meta*-kinked LCPs, are strongly affected by TFPA and TFIA units. TFPA and TFIA moieties with 60 and 120° angular conformations may correspondingly dedicate a twist and bend on a rigid straight polymer chains. The TFPA moiety may create a higher rotation ability because of its *ortho*-linkage (60° angular conformation),

indicating that the polymer chain may coil together easily. There is clear evidence in Fig. 2(b) that *meta*-linkages induce chain flexibility, but at the same time maintain the linearity and straightness of a polymer back bone, which readily forms mesophases.

Fig. 3 depicts that the persistence length of ABA/AAA/TFTA decreases drastically with an increase in temperature. This implies that temperature has a significant effect on chain straightness. As compared to the ABA/AAA/TFTA system, the ABA/AAA/TFPA and ABA/AAA/TFIA systems with *ortho-* and *meta*-linkages have a lower sensitivity of persistence length to temperature, suggesting greater chain entanglement in the kinked systems.

3.2. LC texture evolution and microstructure changes

Figs. 4 and 5 show the evolution of LC texture and microstructure changes during the polymerization of the ABA/AAA/TFPA (*ortho*) ABA/AAA/TFIA (*meta*) and ABA/AAA/TFTA (*para*) systems at different reaction times. All the micrographs were obtained from the same area of the same sample under a polarizing light microscope at 300 °C for 2 h. Using the ABA/AAA/TFPA system (Fig. 4) as an example, in the early stages of LC formation, oligomers formed in the molten monomer phase. The brighter phase that appeared during the early stages of
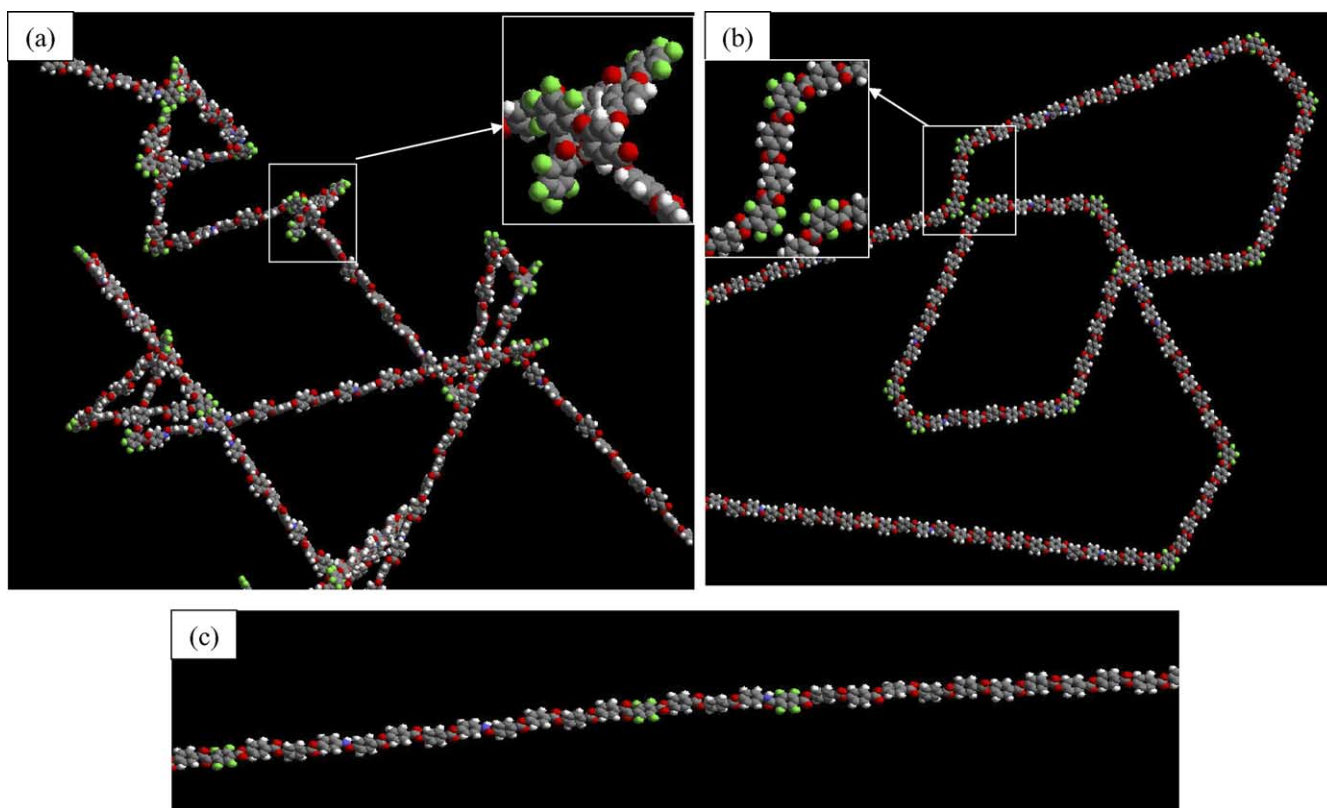

Fig. 2. Set of simulation observed for (a) ABA/AAA/TFPA, (b) ABA/AAA/TFIA and (c) ABA/AAA/TFTA copoly(ester–amide)s with 70/15/15 mol% (300 repeated units), built at 300 °C.

reaction is LC domain, while the darker phase represents the isotropic melt.

Once the minimum requirement of persistence ratio for liquid crystallinity is reached, LC droplets start to appear and separate from the isotopic phase. This is clear evidence that molecular weight and LC chain length increase rapidly with time in the early stages (70–120 s) of polymerization. Subsequently, the generation of LC phase and the coalescence of LC phase take place simultaneously. In general, the coalescence process is faster than the generation of LC droplets. At 156 s, the overall view area becomes an anisotropic phase (i.e. Schlieren texture). After 8 min of polymerization, the crystal phase can be clearly discerned. The crystal structure continues to grow and takes possession of the whole micrograph until the polymerization reaction has continued for 2 h. Similar patterns of LC texture evolution and microstructure changes can be observed in Fig. 5(a) and (b) for the ABA/AAA/TFIA (*meta*) and ABA/AAA/TFTA (*para*) systems. All copolymers underwent the following changes in morphology: generation of LC droplets; coalescence of the LC domains; formation of Schlieren texture, and the annihilation of disclinations. Only crystalline texture was observed at the end of the reaction for all the systems studied.

3.3. Comparison of the effect of the ortho-, meta- and para-linkage on the liquid crystallinity

As shown in Figs. 4 and 5, the incubation period until the appearance of LC phase is strongly dependent on the kink substituents. Previous studies suggested that the formation of liquid crystallinity would follow this sequence: *para-*, *meta-* and lastly *ortho*-linkages [17]. In contrast to the earlier studies, we have observed that the *ortho*-linkage has the shortest time to evolve the LC texture, followed by the *para-* and then the *meta*-linkages. Theoretically, TFPA with a lower persistence ratio is unfavorable to form mesophases. However, its low melting point (162 °C) and its potential to create *cis*-configuration (discussed later) may help induce the LC formation in the early stage of polymerization. The rigidity and straightness of TFTA compensate for the drawback of its highest melting point (275 °C) within the series. The kink structure and relatively high melting point (212 °C) of TFIA may cause the *meta*-linkage system to be the last to form LC texture.

Due to the resonance effect of C=O bond in the backbone, the N–C bond (amide group) may have a double bond character, TFPA with the *ortho*-linkage may undergo a *cis*-configuration and give a 60° angular conformation as compared to those of *meta*-linkage. Based on the previous computer simulation, the energy difference between the *cis*- and *trans*- configuration for PhNH–COPh is very small (2.6 kcal/mol) [30] while the rotational barrier for amide group is relatively large ($\sim$16 kcal/mol) [31]. This indicates that the incorporation of *cis*-configuration may create a side step (crankshaft) effect between AAA and TFPA, and result in an increase in its quasi aspect ratio and local chain rigidity. Even though the *ortho*-linkage can produce the *cis*-configuration, it can also create an unstable conformation and configuration if the *ortho* content is high. This is due to the fact that the coexistence of *cis* and *trans*-configurations in random polymerization may result in a reduction of overall aspect ratio, linearity and chain rigidity. In other words, the *cis*-configuration would occur and enhance local chain rigidity (liquid crystallinity) in the early stage of polymerization if the TFPA content is low.

Fig. 6 illustrates the evolution of LC area as a function of time during the thin-film polymerization. There seems to
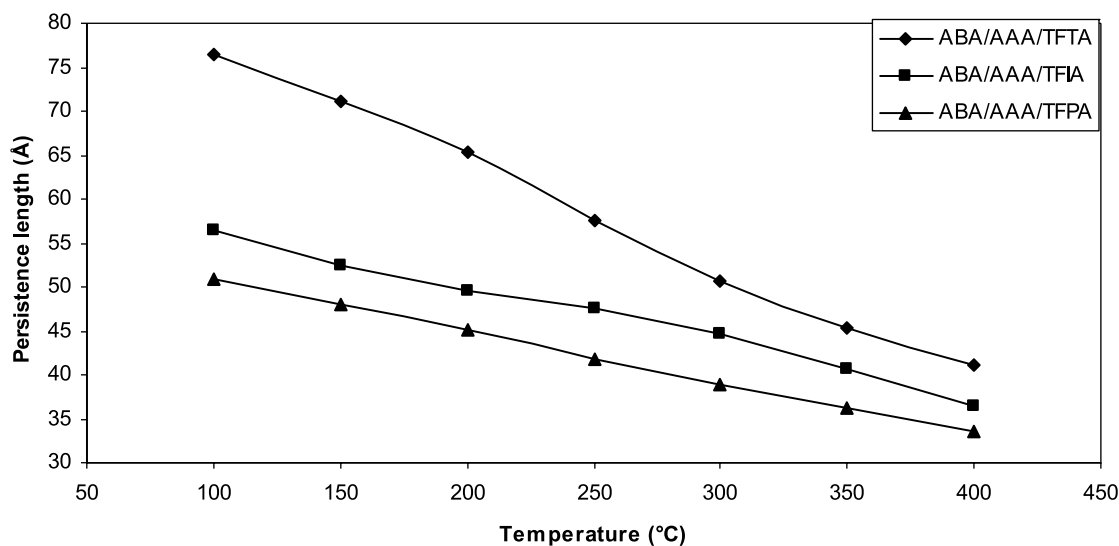
Fig. 3. Calculated temperature dependence of the persistence length for 70/15/15 ABA/AAA/TFPA, ABA/AAA/TFIA, and ABA/AAA/TFTA systems by simulation.
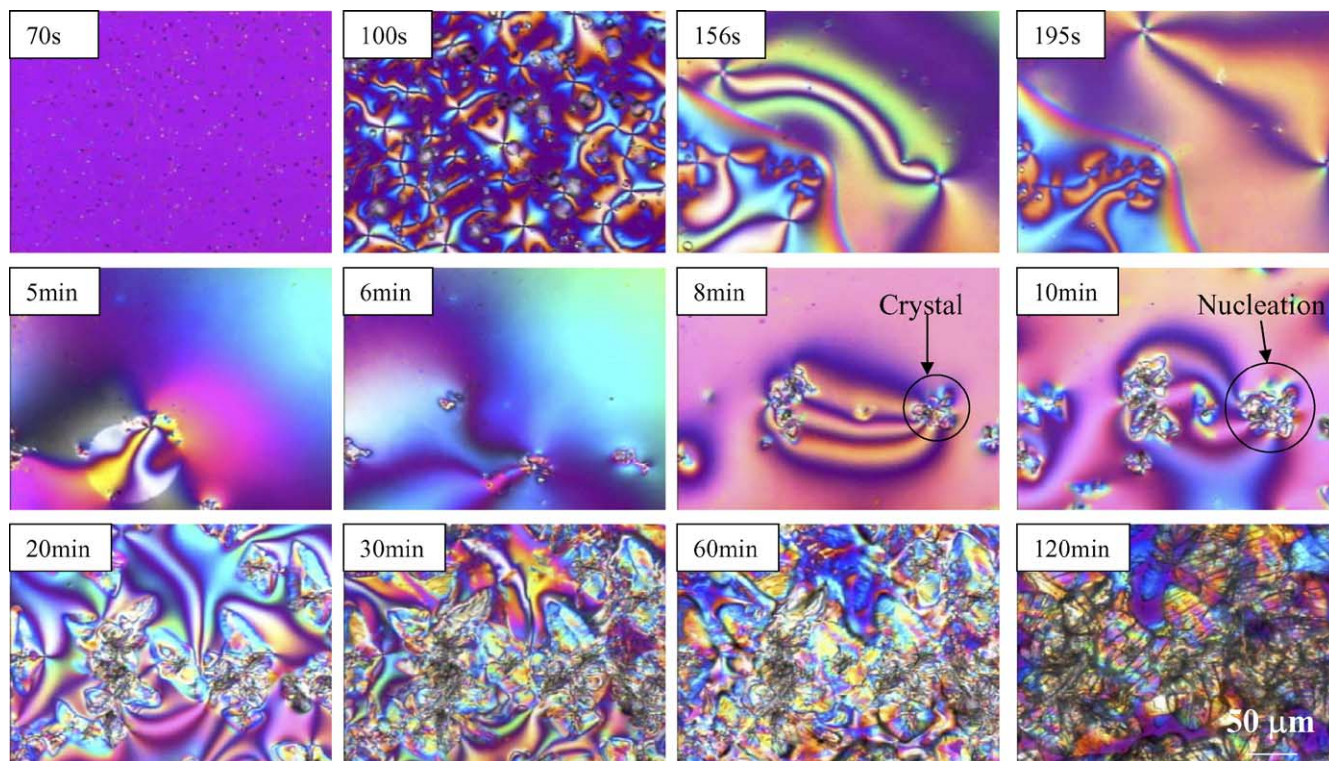
Fig. 4. Morphology of the 70/15/15 ABA/AAA/TFPA (*ortho*) polymerization reaction system at different reaction times. All the micrographs were obtained from the same area of the same sample. Reaction temperature: 300 °C.

have two stages for the LC growth. The initial stage corresponds to individual domain growth, while the second stage corresponds to aggregated domain growth through various annihilation processes. Because the *meta*-linkage system has a slower LC growth rate, it has a clear transition from individual to aggregated domain growth. This phenomenon may also arise from the fact that the *meta*-linkage system may have relatively higher viscosity or lower elastic constants than the other two systems. Another possible explanation is that the rigid TFIA (*meta*) moiety may require a much longer time to undergo the *cis*-configuration (discussed later).

Even though these fluorinated moieties have different conformations and configurations, they yield similar end-stage morphology. Only crystalline structure has been observed from the resultant copolymers. As shown in Fig. 4, the crystallinity grown from the LC phase develops through spherulitic growth and then by the nucleation process [32]. Usually, these spherulites are grown from the dark brushes around a single disclination, indicating that these are the lowest energy for crystallization. Fig. 7 demonstrates the evolution of their crystalline areas as a function of time. The crystallinity grows in three stages. The first stage (from the crystalline formation to about 30 min) is rapid, then slows down and further slows down after 60–70 min. TFPA system is the first to develop crystal texture, but its growth rate quickly decreases in the later stage of polymerization (at about 62 min). This may be due to the

difficulties of inducing chain folding for the *ortho*-linkage system because of the coexistence of *cis*- and *trans*-configurations.

3.4. The critical ABA content for the LC formation

3.4.1. Comparison between ABA/AAA/TFPA, ABA/AAA/TFIA, ABA/AAA/TFTA systems

The critical (or the minimum) ABA content to form the LC phase was determined and shown in Figs. 8 and 9. Consistent with the previous simulation, the ABA/AAA/TFTA (*para*) system requires the lowest ABA content for LCs texture formation because the *para*-linkage has greater chain straightness and tendency for liquid crystallinity. For example, 15 mol% of ABA is required in the ABA/AAA/TFTA system at 300 °C while 40 mol% of ABA is necessary in the ABA/AAA/TFPA system (as shown in Fig. 8). Above the critical content, higher ABA critical content means higher rates of LC formation; while below the critical content, only isotropic or crystal phase are found. In addition, these figures also suggest that a higher reaction temperature results in a lower critical ABA content. One possible reason is that high temperature probably leads to the rapid increase in molecular weight and persistence ratio. As a consequence, for the same composition, a higher reaction temperature usually results in an easier and faster formation of LC phase.

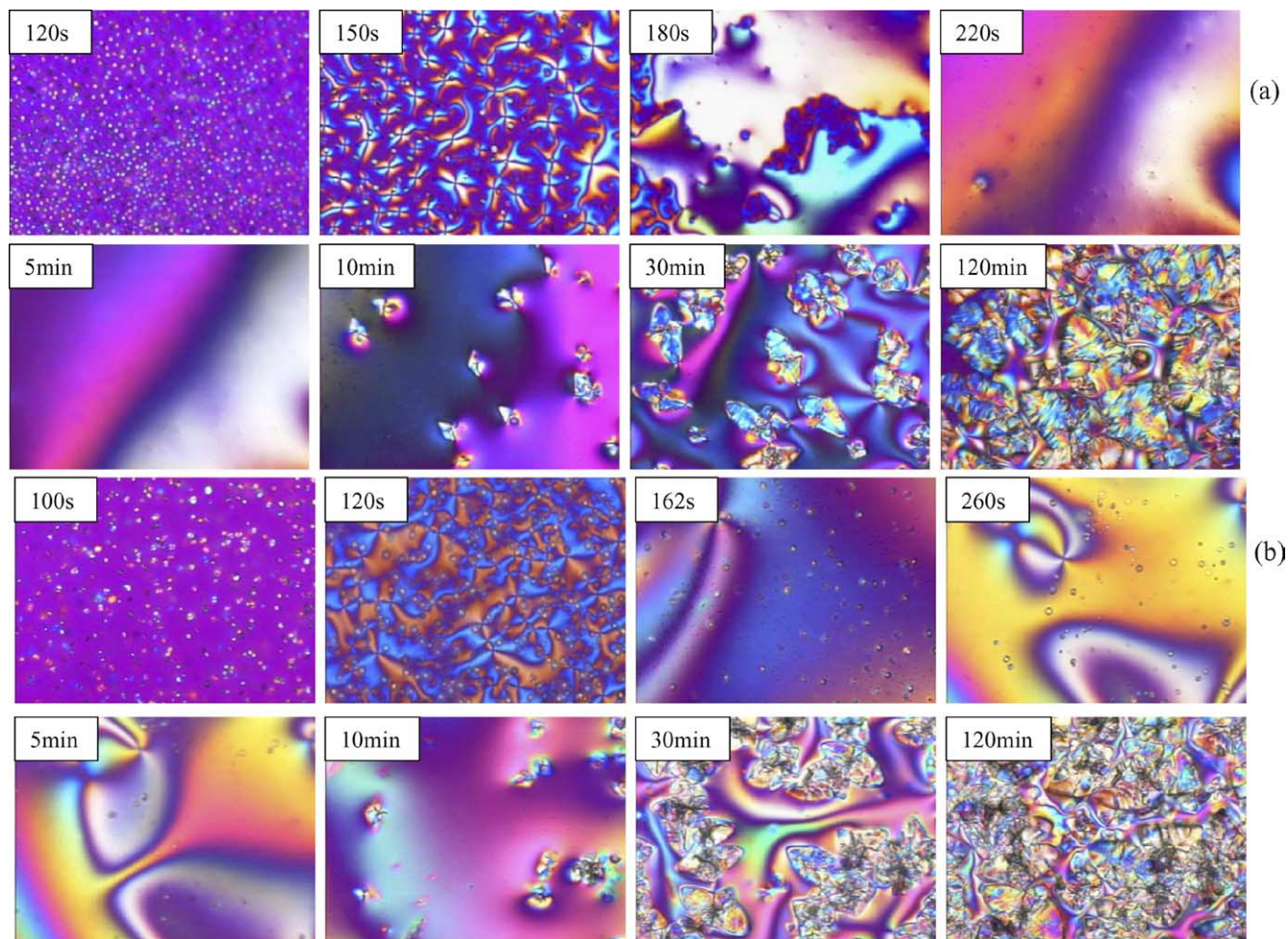As illustrated in Fig. 8, the experimental data show that

Fig. 5. Morphology of the 70/15/15 (a) ABA/AAA/TFIA (*meta*) and (b) ABA/AAA/TFTA (*para*) polymerization reaction system at different reaction times. All the micrographs were obtained from the same area of the same sample. Reaction temperature: 300 °C.
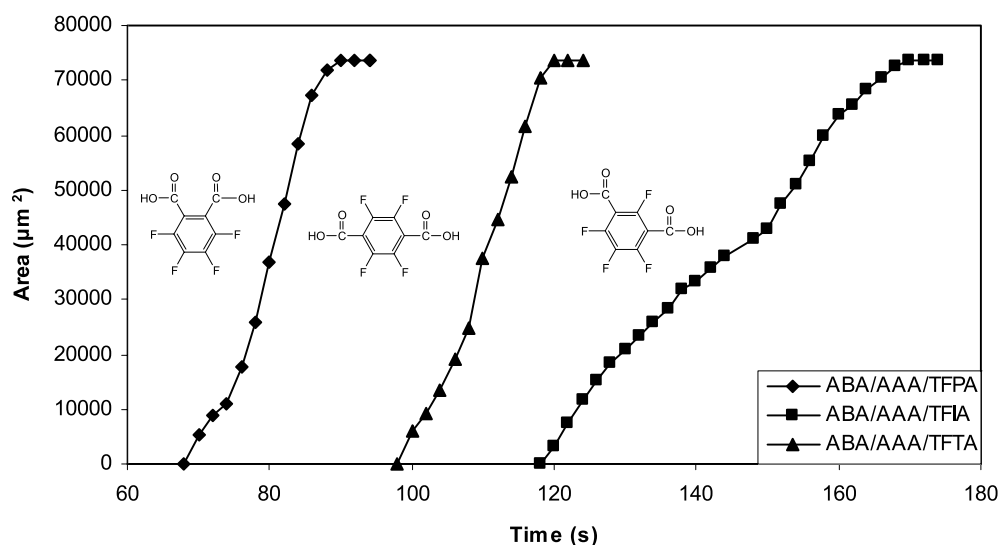

Fig. 6. Time dependence of the area (A) of the LC annihilation process for 70/15/15 ABA/AAA/TFPA (TFIA/TFTA) systems at 300 °C.
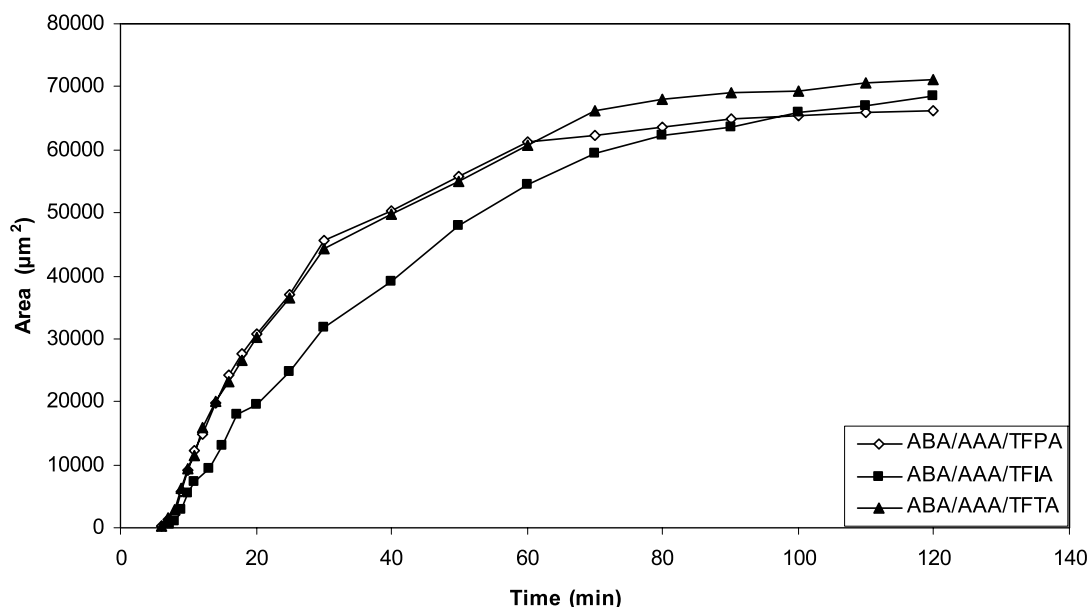
Fig. 7. Time dependence of the area (A) of the crystal growth process for 70/15/15 ABA/AAA/TFPA (TFIA/TFTA) systems at 300 °C.

the ABA/AAA/TFPA (*ortho*) system has a lower tendency to yield the LC phase than either the ABA/AAA/TFIA (*meta*) or ABA/AAA/TFTA (*para*) systems, matching with the simulation results in Table 1. These data suggest that the *ortho*-linkage has poor intra- and intermolecular attractive force as compared to the *meta*-linkage because of poor intrinsic rotation potential around the bond and the steric hindrance to rotate among intermolecular chains due to non-bonded interaction. Once TFPA content reaches 26–31 mol%, the liquid crystallinity is disrupted dramatically.

On the other hand, TFIA with its *meta*-linkage has a much higher tendency to form LC than TFPA. One plausible explanation is due to the fact that some of the ester linkages in ABA/AAA/TFIA may assume a *cis*-configuration that facilitates the formation of liquid crystallinity. Although TFIA with 120° angular conformation cannot induce a crankshaft effect, its may form a *cis*-configuration by the

ester linkage. Computer simulation shows the energy difference for ester (8 kcal/mol) is higher than the amide (2.6 kcal/mol) [30]. As a result, the ester group is conceptually more difficult to form a *cis*-configuration than the amide group. However, if the polymer chain can exhibit the energy requirement for an ester linkage *cis*-configuration, the polymer may have a higher persistence length and symmetry structure, leading to a more stable LC structure.

Although a *meta* system can exhibit the *cis*-configuration, it may take a much longer time to overcome the higher energy difference for the formation of ester linkages. In addition, the resultant polymers could achieve close regular packing in the liquid crystalline region, which is similar to a straight chain in *para*-linkage (matching the chain conformation as shown in Fig. 2(b)). Therefore, both *meta*- and *para*-linkage systems have close critical ABA content as shown in Fig. 8. At 360 °C, the *meta*-linkage
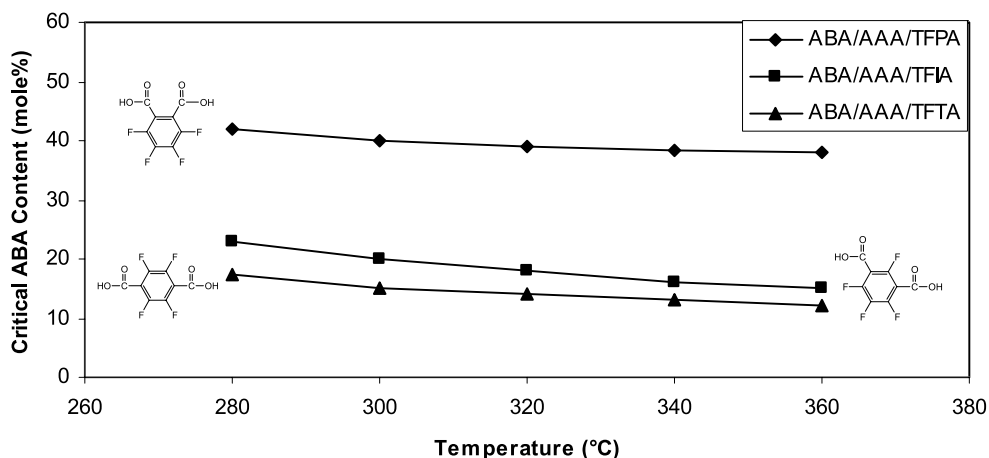

Fig. 8. The dependence of the critical ABA content for ABA/AAA/TFPA, ABA/AAA/TFIA and ABA/AAA/TFTA systems on the reaction temperature.
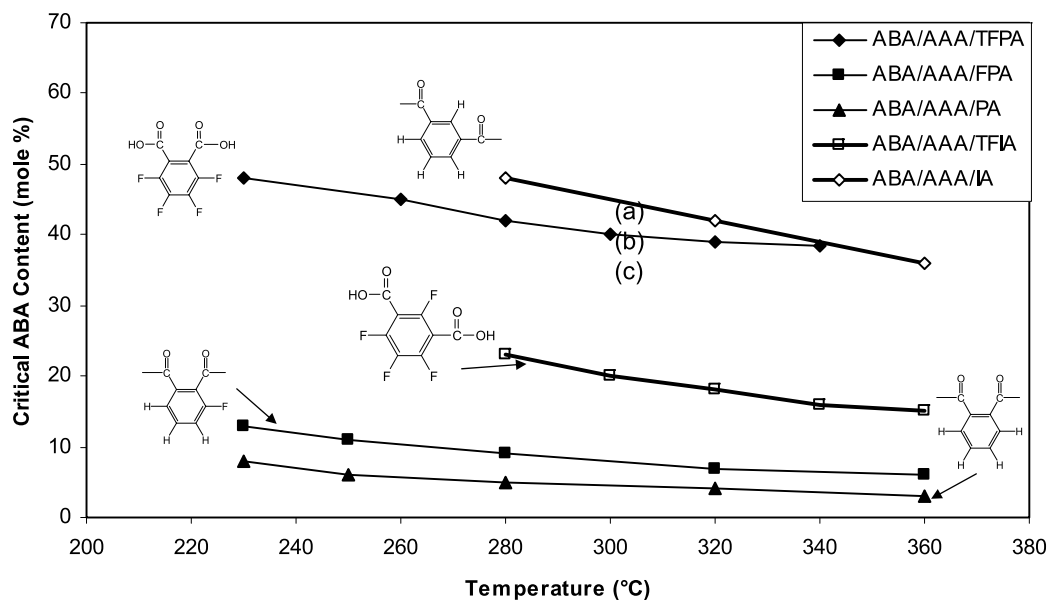
Fig. 9. The dependence of the critical ABA content for ABA/AAA/TFPA, ABAAAA/FPA [19], ABA/AAA/PA [19], ABA/AAA/TFIA and ABA/AAA/IA [16] systems as a function of reaction temperature.
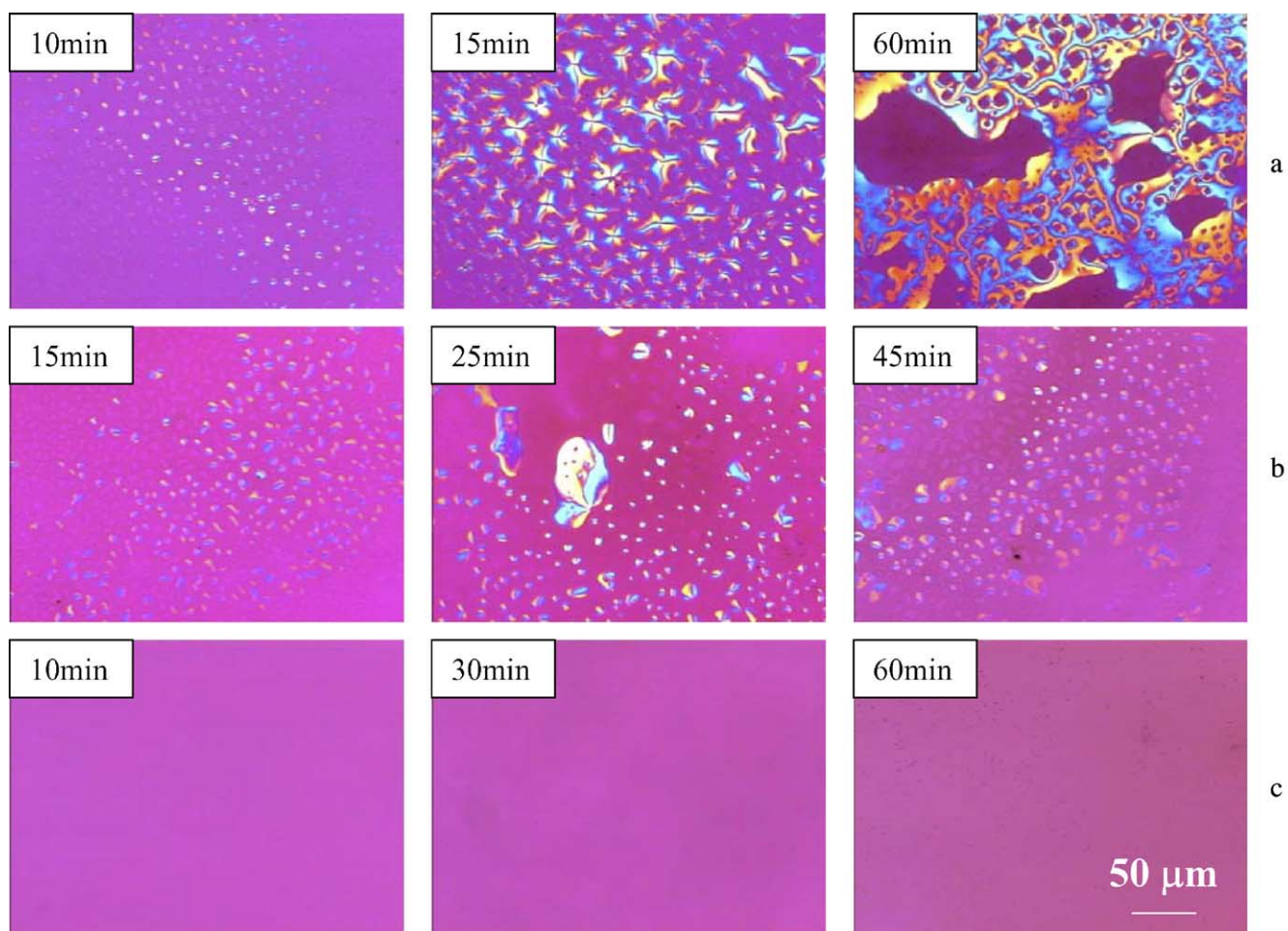

Fig. 10. Morphology of the ABA/AAA/TFPA polymerization reaction system at different reaction compositions: (a) 45/27.5/27.5, (b) 40/30/30, (c) 30/35/35. All the micrographs were obtained from the same area of the same sample. Reaction temperature: 300 °C.
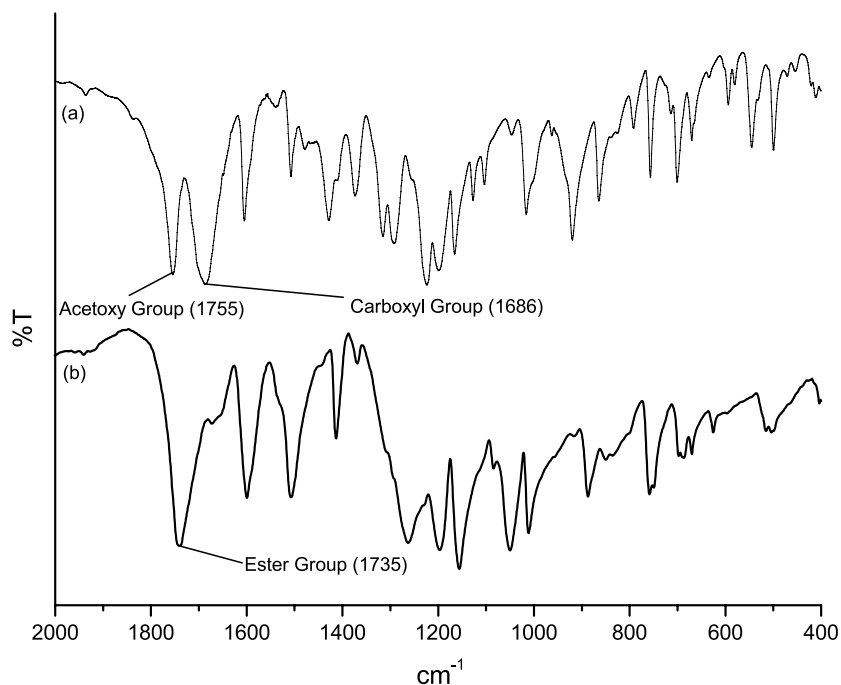
Fig. 11. The FT-IR spectra of 70/15/15 ABA/AAA/TFIA reaction system at 300 °C for different reaction times: (a) 0 min, and (b) 2 h.

system can tolerate 42.5 mol% of TFIA moiety, while the *para*-linkage system can stand 44 mol% of TFTA moiety before loosing LC characteristics.

3.4.2. Comparison between ABA/AAA/TFPA, ABA/AAA/TPA, ABA/AAA/PA, ABA/AAA/TFIA and ABA/AAA/IA systems

From Fig. 9, it is evident that the fluorine substituent plays an important role in the formation of liquid crystallinity. The effects of a fluorine lateral moiety on the liquid crystallinity of fluorinated aromatic [18–19] and also perfluoroalkyl aliphatic poly(ester–amide)s systems have been previously reported [20]. According to Cheng and Chung [19], the fluorine lateral moiety has an unfavorable effect on the annihilation reaction. The LC formation in the current ABA/AAA/TFPA system appears to have a similarity to those studies observed in the poly(ester–amide)s system. This finding clearly reflects that the replacement of a hydrogen atom by a fluorine atom has a huge effect on the requirement of critical ABA mol%. The fluorine atom has a much higher atomic weight, but it is only 10% larger in van der Waals radius than hydrogen. Thus, the packing density of the fluorocarbon far exceeds that of the hydrocarbon moiety. The ABA/AAA/FPA system, which has only one fluorine substituent on the aromatic ring, has a similar liquid crystalline behavior to that of the fluorine-free ABA/AAA/PA system.

When phthalic acid (PA) or 3-fluorophthalic acid (TFA) units are replaced by the TFPA unit, with four fluorine atoms, the lowest critical ABA content is observed in Fig. 9. According to a previous report [33], the introduction of large fluorine–fluorine repulsions in a polymer backbone

has been shown to decrease the phase transition temperature of thermotropic LCPs, and generally leads to the transition from the isotropic to nematic stage. Thus, the TFPA is expected to have lower critical ABA content than TPA and PA at the same reaction temperature. However, the current results show a contrasting feature of these copolymers. A plausible explanation for this alternative behavior is that fluorine atoms have a higher polarity and electronegativity affect in the *ortho*-position which destroys the liquid crystal stability when the content is high. In other words, the ability of *ortho*-linked aromatic poly(ester–amide)s to form stable thermotropic LCPs appears to depend on the particular extent of its incorporation.

On the other hand, when comparing the requirements of critical ABA content between ABA/AAA/TFIA and ABA/AAA/IA (isophthalic acid) systems, surprisingly, we observed that the former has a much lower critical ABA content than the latter. If the *meta*-linkage moiety could induce the liquid crystallinity because of forming a *cis*-configuration at its ester linkage; the four fluorine substituent atoms of TFIA definitely help chain rigidity and stabilize the LC mesogens because of their high polarity and electronegativity, and unique configuration (i.e. ring substitution). As a result, 18 mol% ABA is required in the ABA/AAA/TFIA system at 320 °C, while 42 mol% ABA is necessitated in the ABA/AAA/IA system. Yet, the introduction of fluorine content has resulted in an unfavorable LC characteristic in the *ortho*-linkage while having higher potential in the *meta*-linkage.

The morphology of the ABA/AAA/TFPA polymerization reaction system at different reaction compositions: (a) 45/27.5/27.5 (above critical content), (b) 40/30/30, (on the

Table 2

The thermal behavior observed by DSC and TGA examination for copoly(ester–amide)s LCPs

	TFPA (*ortho*)	TFIA (*meta*)	TFTA (*para*)
Melting Point, T_m (°C)	Nil	335	334
Crystallization Point, T_d (°C)	256	291	284
Degradation temperature, T_d (°C)	401	352	381

critical content) and (c) 30/35/35 (below critical content) are shown in Fig. 10 and their relative positions are labeled in Fig. 9. Compared to the 45/27.5/27.5 ABA/AAA/TFPA system, the 40/30/30 ABA/AAA/TFPA system has much a slower LC growth process during the early stages of reaction. By further decreasing the ABA content, only the amorphous phase is found during the entire stage of polymerization. This is probably due to the random distribution of short rigid chain segments which makes them difficult to crystallize or form mesophase.

3.5. Characterization

To show that the fluorine substituent moieties have been successfully incorporated into the LCPs chains, FT-IR was used to identify the individual chemical functionalities. Two representative samples, the monomer mixture and the LCPs that had been in situ polymerized for 2 h, were chosen. The FT-IR spectra of monomers and copoly(ester–amide)s for the 70/15/15 ABA/AAA/TFIA system were characterized as a function of reaction time and shown in Fig. 11. The bands at 1755 and 1686 cm^{-1} correspond to the $v_{C=O}$ of CH$_3$COO– and $v_{C=O}$ of –COOH, respectively. These bands were observed to almost completely disappear with completion of the reaction. When the polycondensation reaction was continued at 300 °C for 2 h, a new band of ester group at 1735 cm^{-1} was formed, clearly indicating the formation of a copolymer.

DSC and TGA were employed to study the copolymer thermal behavior. The typical DSC heating and cooling traces of ABA/AAA/TFTA system were studied at a rate of 20 °C/min between 50 and 360 °C. Usually, the melting points for the first generation LCPs were observed to be between 350 and 450 °C, which is not convenient for conventional processing facilities. Therefore, one of the major objectives in thermotropic LCP research has been to

reduce the transition temperature to ideally less than 300 °C [2]. In Table 2, it is noted that from the DSC examination, the melting point (T_m) for the ABA/AAA/TFIA (*meta*) and ABA/AAA/TFTA (*para*) systems are 335 and 334 °C, which may still be in an acceptable processing temperature range. The TGA examination has suggested that the degradation temperature (T_d) for the ABA/AAA/TFPA, ABA/AAA/TFIA and ABA/AAA/TFTA systems at a 5% weight loss were 401, 352 and 381 °C, respectively.

4. Conclusions

The influence of fluorinated kinked moiety units on the polymer properties, thermal properties, liquid-crystalline behavior, and degree of crystallinity were investigated. The likelihood of LC texture formation was supported by molecular science simulation and confirmed by thin film polymerization. From the metropolis Monte Carlo simulation, all systems met the minimum persistence ratio requirement (6.42) for LC evolution.

Experimental and simulation results propose that the *para*-linkage (TFTA) is the most favorable system to form the LC phases because of higher persistence ratio, linearity and chain straightness. In the early stage of polymerization, TFPA (*ortho*) copolymer most readily produces LC phases due to its low melting point (162 °C) and potential to create a crankshaft structure, induced by *cis*-configuration between AAA and TFPA moieties. Although the *meta*-linkage system is the last to form LC domain, it has a much higher tendency to yield mesophase than the *ortho* system. Thus, *ortho*-substituted copolymers enjoy a kinetic advantage over *meta*-substituted systems in forming mesophases, but thermodynamics favors *meta* over *ortho*.

For ABA/AAA/TFIA and ABA/AAA/IA (isophthalic acid) reaction systems, the former surprisingly exhibits a

much lower critical ABA content than the latter; the four fluorine substituents of TFIA contribute to chain rigidity and stabilize the LC mesogens. Conversely, when comparing the ABA/AAA/PA and ABA/AA/TFPA systems, replacement of hydrogen atom (PA) by four fluorine substituents (TFPA) in *ortho*-linked copolymers results in a dramatic loose of LC character. The fluorine substituents in the *ortho*-position have a higher polarity and electronegativity which destroy the stability of liquid crystal phases.

Acknowledgements

References

[1] Plate NA. Liquid crystal polymers. New York: Plenum Press; 1993.
[2] Chung TS. Thermotropic liquid crystal polymers—thin-film polymerization, characterization, blend and application. New York: CRC press; 2001.
[3] Collyer AA. Liquid crystal polymers: from structure to application. London: Elsevier; 1992.
[4] Chung TS. Polym Eng Sci 1986;26:901–19.
[5] Silverstein MS, Hiltner A, Baer E. J Appl Polym Sci 1991;43:157–73.
[6] Donald AM, Windle AH. Liquid crystalline polymers. Cambridge: Cambridge University Press; 1992. p. 50–125.
[7] Wang Y, Xu JM, Cheng SX, Pramoda KP, Chung TS, Goh SH. Liq Cryst 2003;30:753–64.
[8] He CB, Lu ZH, Zhao L, Chung TS. J Polym Sci Polym Chem 2001; 39:1242–8.
[9] Chen BQ, Kameyama A, Nishikubo T. J Polym Sci Polym Chem 2000;38:988–98.
[10] Bicerano J. Comput Theor Polym Sci 1998;8:9–13.
[11] Foulger SH, Rutledge GC. J Polym Sci Polym Phys 1998;36:727–41.
[12] Bladon P, Frenkel D. J Phys: Condens Matter 1996;8:9445–9.
[13] Krigbaum WR, Brelsford G, Ciferri A. Macromolecules 1989;22: 2487–91.
[14] Shibaev VP, Lam L. Liquid crystalline and mesomorphic polymers. New York: Springer; 1994.
[15] Flory PJ, Ronca G. Mol Cryst Liq Cryst 1979;54:311.
[16] Cheng SX, Chung TS, Mullickof S. J Polym Sci Polym Phys 1999;37: 3084–96.
[17] Cheng SX, Chung TS. J Polym Sci Polym Phys 2000;38:2221–31.
[18] Chung TS, Ma KX, Cheng SX. Macromol Rapid Commun 2001;22: 835–41.
[19] Cheng SX, Chung TS. Polymer 2002;43:7433–41.
[20] Teoh MM, Chung TS, Cheng SX, Lin TT, Pramoda KP. Liq Cryst 2004;31:871–81.
[21] Liu XH, Manners I, Bruce DW. J Mater Chem 1998;8:1555.
[22] Ishikawa H, Toda A, Okada H, Onnagawa H. Liq Cryst 1997;22: 743–7.
[23] Liu JG, Li ZX, Wu JT, Zhou HW, Wang FS, Yang SY. J Polym Sci Polym Chem 2002;40:1583–93.
[24] Wewerka K, Wewerka A, Stelzer F, Gallot B, Andruzzi L, Galli G. Macromal Rapid Commun 2003;25:906–10.
[25] Percec V, Glodde M, Johansson G, Balagurusamy VSK, Heiney PA. Communications 2002;42:4338–42.
[26] Xiang M, Li X, Ober CK, Char K, Genzer J, Sivaniah E, et al. Macromolecules 2000;33:6106–19.
[27] Cerius^2 simulation tool user's reference, molecular simulations software for material science. San Diego, CA: Molecular Simulation Inc; 1996.
[28] Windle AH. In: Shibaev VP, Lam L, editors. Liquid crystalline and mesomorphic polymers. New York: Springer; 1994.
[29] Chung TS, Calundann GW, East AJ. Liquid crystalline polymers and their application. Encyclopedia of engineering materials. vol. 2. New York: Marcel Dekker; 1989. p. 625.
[30] He CB, Windle AH. Marcomol Theory Simul 1995;4:289–304.
[31] Chung TS, Cheng M, Pramoda KP, Goh SH. Polym Eng Sci 1999;39: 953.
[32] Hadershi D, Nazarenko S, Cheng CM, Hiltner A, Baer E. Macromol Chem Phys 1995;196:2545–61.
[33] Ueda M, Noguchi Y, Sugiyama J, Yonetake K, Masuko T. Macromolecules 1992;25:7089.